# Evidence for in-plane spin-flop orientation at the MnPt/Fe(100) interface revealed by x-ray magnetic linear dichroism

J. Fujii,[1] F. Borgatti,[1] G. Panaccione,[1,*] M. Hochstrasser,[2] F. Maccherozzi,[1] G. Rossi,[3] and G. van der Laan[4]
[1]*Laboratorio TASC-INFM CNR, Basovizza, S.S. 14, km 163.5, 34012 Trieste, Italy*
[2]*Laboratorium für Festkörperphysik, Wolfgang-Pauli-Strasse 16, ETH Hönggerberg, CH-8093 Zürich, Switzerland*
[3]*Dipartimento di Fisica, Università di Modena e Reggio Emilia, via Campi, Modena, Italy*
[4]*Magnetic Spectroscopy, Daresbury Laboratory, Warrington WA4 4AD, United Kingdom*
(Received 22 February 2006; revised manuscript received 25 May 2006; published 28 June 2006)

X-ray magnetic linear and circular dichroism at the Mn $L_{2,3}$ edges are used to determine the magnetic properties of epitaxial MnPt films on Fe(100). The good agreement between experimental linear dichroism and multiplet calculations reveals that the Mn spins are aligned in plane but perpendicularly to the underlying in-plane Fe spins. The absence of magnetic circular dichroism rules out the presence of uncompensated Mn spins at the interface.

DOI: 10.1103/PhysRevB.73.214444 PACS number(s): 75.25.+z, 75.30.Et, 75.70.Rf

## I. INTRODUCTION

The exchange bias effect is currently of great interest because of its application for magnetic devices with spin valves and magnetic tunnel junctions,[1,2] where the local magnetic structure at the antiferromagnet/ferromagnet (AFM/FM) interface plays a key role.[3–9] The observation of pinned spins at the AFM/FM interface was recently reported for polycrystalline sandwiches used in room-temperature device structures,[10] including metallic or insulating AFM materials. It has been speculated that the origin of the uncompensated pinned spins resides at the grain boundaries and that the size of their contribution can quantitatively explain the macroscopic exhange bias using a simple model.[11,12] The relationship between crystallographic direction and magnetization reversal, due to the influence of the unidirectional anisotropy, has been recently addressed in MnPd films.[13] Exchange bias effects have been observed for polycrystalline MnPt thin film when the bilayer was made with FeNi or FeCo.[14] Recent experiments on MnPt/NiFe exchange-biased bilayers grown by molecular beam epitaxy have shown that the magnetic moments might be antiferromagnetically aligned parallel or normal to the interface.[15–17] The delicate interplay of interfacial magnetism with chemical and structural order has been recently demonstrated in the epitaxial growth of Fe/twinned MnPt bilayers studied by the magneto-optical Kerr effect.[18] In spite of extensive experimental and theoretical research the basic mechanism of this effect is still unclear, and a better control of the factors affecting the AFM/FM interface formation is highly desired. With this aim, the detailed study of AFM/FM interfaces developed by epitaxy-based techniques is important for the understanding of the interfacial effects on magnetic properties.

In this work we investigated the magnetic structure of a thin MnPt film with well-defined phase and thickness grown by molecular beam epitaxy on the Fe(100) interface with use of x-ray absorption spectroscopy (XAS) and x-ray magnetic linear and circular dichroism (XMLD and XMCD) at the Mn and Fe $L_{2,3}$ edges. These techniques merge element and chemical sensitivity with the information about the distribution of the magnetic moments. MnPt is an antiferromagnetic AuCu-I type ordered alloy with a magnetic moment of $4.3\mu_B$ (Ref. 19) and Néel temperature of 970 K, which makes it — and similar alloys like MnPd and MnIr — appealing materials to act as a pinning layer for giant-magnetoresistance (GMR) devices. The MnPt tetragonal structure has lattice parameters $a=4.00$ Å and $c/a=0.92$, hence Fe(100) is a very good candidate for epitaxial growth because its lattice parameter (2.87 Å) favors a small mismatch of 1.5% with the overlayer oriented with the $a$ axis along the Fe{110} direction and the $c$ axis perpendicular to the Fe(100) surface. In this experiment we find a clear XMLD signal at the Mn edges for in-plane sample magnetization indicating that the Mn magnetic moments are antiferromagnetically oriented parallel to the surface. The measurements are compared with multiplet calculations to obtain information about the ground-state properties of the system. It turns out that the Mn XMLD is related to AFM domains aligned *perpendicularly* to the Fe[001] magnetization axis, leading to spin-flop AFM ordering parallel to the surface, whereas the AFM domains of bulk MnPt are usually oriented along the $c$ axis. The interface exhibits uniaxial magnetic anisotropy without exchange bias. The absence of any Mn XMCD signal excludes the presence of uncompensated Mn spins at the interface, while the substrate maintains its single-domain ferromagnetic structure.

## II. EXPERIMENTAL SETUP

The measurements were performed at room temperature on the APE undulator beamline at the Elettra synchrotron radiation facility. The Fe(3% Si) (100) single crystal was prepared through repeated cycles of $Ar^+$ sputtering and annealing at 400 °C. The presence of Si, C, and P segregated impurities, as revealed by Auger electron spectroscopy, was further confirmed by the sharp $c(2\times2)$ low-energy electron diffraction (LEED) patterns.[20] An 8 monolayer (ML) thick MnPt film was grown on Fe(100) by *in situ* coevaporation. The base pressure in the sample preparation chamber was $4\times10^{-11}$ mbar and during deposition the pressure remained below $2\times10^{-10}$ mbar. After the deposition the Fe Auger peaks retain a sizable intensity and we observe a $(1\times1)$

 

LEED pattern, thus confirming that the MnPt grows with the *c* axis perpendicular to the surface. After the deposition, Si and C disappeared from the Auger spectra and only a small residual (<0.1 ML) P remains, indicating that Si and C are not present in the MnPt film. In order to prevent oxidation the film was capped with 4 ML Pt. Magnetic dichroism measurements were done with the sample magnetized in plane at remanence. The spot size was of the order of 120 $\mu$m. The absorption spectra were recorded by collecting the total electron yield (TEY). For normal incidence XMLD the x-ray beam polarization was fixed and the sample was rotated about the surface normal, to obtain $E_\pi$ ($E_\sigma$) parallel (perpendicular) to $M$, where $E$ is the linear polarization direction of the light and $M$ is the substrate magnetization directed along the Fe[001] axis. We also recorded the spectra with the sample rotated around the normal by 180°. The final results are averaged over the two data sets. The XMCD was detected with incidence angle 45° along the Fe[001] direction and by averaging on the spectra collected by swapping the magnetic field and the right (left) circular polarization. Characterization of the Fe(100) magnetic ordering before MnPt deposition was performed by XMCD and spin-polarized measurements. The spin polarization of the secondary electrons ejected from the iron surface was measured with two 60 kV Mott scattering polarimeters[21–23] mounted at 90° with respect to each other. The detection of the secondary electrons in the Mott scattering experiments gives a spin-polarization value proportional to the averaged surface magnetization of the sample.[24]

## III. RESULTS AND DISCUSSION

One advantage of growing AFM layers over a FM substrate is that the latter can be magnetized to achieve a single domain large enough to investigate the AFM-FM coupling without using microscopy. In our experiment the typical size of the ferromagnetic domains of the Fe(100) substrate was 0.5 mm, as revealed in Fig. 1 by XMCD and spin-polarization measurements recorded by scanning the beam position over the same sample surface in the same experimental run. The XMCD image was obtained in TEY mode by fixing the photon energy at the Fe $L_3$ edge, i.e., at the maximum of the dichroic signal. There is a remarkable agreement between both XMCD [Fig. 1(a)] and in-plane spin polarized measurements [Fig. 1(b)], both confirming the single-domain surface magnetization along the Fe[001] direction (look at the picture in the inset) whereas any contribution along the [010] direction is absent [Fig. 1(c)].

The Mn $L_{2,3}$ XAS of the 8 ML MnPt film capped with 4 ML Pt is shown in Fig. 2. The most remarkable features of the spectrum are the distinctly split structure of the $L_2$ edge and the two weak shoulders in the high-energy tail of $L_3$. A similar behavior has been observed for 3*d* metals with reduced coordination number, such as for submonolayer deposition of Mn on Cu, Fe and Ni,[25–27] where the 3*d* orbitals are more localized than in the bulk. Our sample is a thin layer containing only four bilayers of alternating Mn and Pt layers, which suggests that, although the system is an intermetallic alloy, the Mn 3*d* states have some degree of electron correlation. The spectrum is compared with the one recorded from a thin Mn film (8 ML) grown on Fe with identical experimental conditions in order to verify the absence of any contamination during the deposition, because the double-peak structure of the $L_2$ peak and the shoulders for $L_3$ could be due to the presence of Mn oxide. The featureless spectrum of the

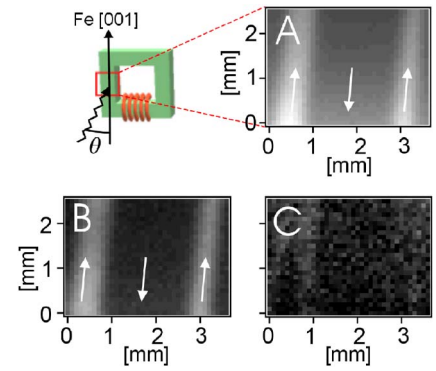


FIG. 1. (Color online) Fe(100) picture frame detected by scanning the sample under the beam. The sample shape and the scanned area are reported in the picture. The in-plane remanence magnetization is oriented along the Fe[001] direction. (a) is the TEY difference (XMCD) for fixed photon energy at the $L_3$ edge maximum absorption. (b) and (c) show the in-plane spin-polarized measurements along the Fe [001] and [010] directions, respectively. White and dark areas correspond to different Fe domains whose orientation along the [001] direction is indicated by the arrows. Both techniques show the presence of single domains at least of the order of 0.5 mm.

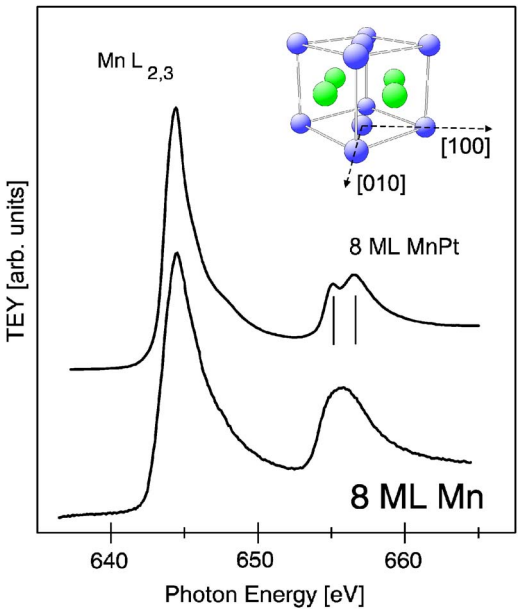


FIG. 2. (Color online) X-ray absorption spectra of 8 ML MnPt/Fe(100) and 8 ML Mn/Fe(100). The spectra are normalized to the $L_3$ peak maximum and shifted vertically for clarity. Both spectra were taken with x rays at normal incidence to the surface. The conventional cell of epitaxial MnPt is rotated by 45° with respect to the {100} surface directions of the underlying Fe substrate, as shown in the inset.

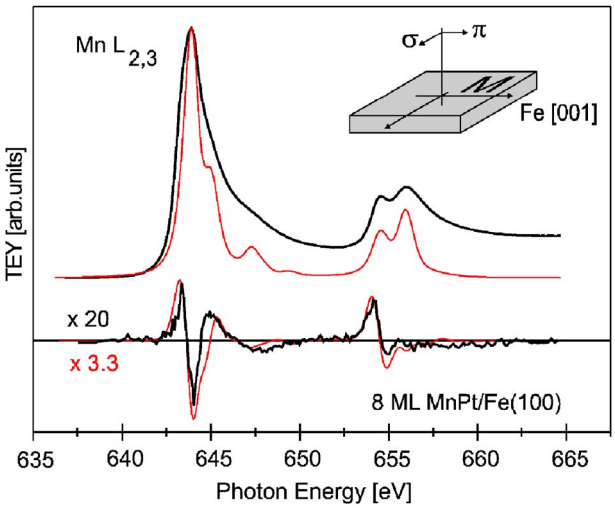


FIG. 3. (Color online) XAS (top) and XMLD (bottom) spectra for 8 ML MnPt/Fe(100) compared to calculations [thin (red) lines]. The inset depicts the experimental geometry, showing the Fe[001] magnetization axis. The sample was in-plane magnetized at remanence. The orientation of the linear polarization with respect to the magnetization is indicated by $\pi$ (parallel) and $\sigma$ (perpendicular). The XMLD is the difference $E_\sigma - E_\pi$.

pure metallic Mn makes us confident that the double-peak structure of $L_2$ in MnPt is not caused by contamination.

We measured the Mn $L_{2,3}$ XMLD both for normal incidence and at grazing angle. The dichroism is always in the order of 1%. Figure 3 shows the isotropic spectrum and the linear dichroism (signal $\times 20$) for normal incidence. The presence of an XMLD signal means that the magnetic ordering of the Mn atoms is antiferromagnetic. For comparison with the experimental results Fig. 3 also shows the XAS and XMLD spectra calculated with atomic multiplet theory in intermediate coupling using Cowan's *ab initio* Hartree-Fock code with relativistic correction[28] and in the presence of crystal field. Details of the calculations can be found in Refs. 29 and 30. A small octahedral crystal field of $10Dq = 0.15$ eV is needed to obtain a line shape of the XMLD compatible with experimental data. A larger crystal field gives a less good agreement, which proves that we are not dealing with an oxide, which would have a crystal field larger than 1 eV. The calculated spectra are normalized to the Mn $L_3$ peak maximum. Comparison of the experimental spectra with calculations is essential to determine the spin axis.[31] In fact, the calculated XMLD spectrum agrees with the experimental curve only for the case that the AFM domains are aligned perpendicularly to the Fe magnetization axis, thus providing evidence for in-plane spin-flop of the Mn magnetic moments, in contrast with the typical AFM orientation of bulk MnPt along the $c$ axis (the [001] direction of the conventional cell, which in our case is perpendicular to the surface). The presence of axial anisotropy perpendicular to the magnetization also differs from a recent XMLD study on a single Mn layer deposited on Fe(100), where the entire noncollinear magnetic structure of Mn is perpendicular to the interface.[32]

We also measured the Mn $L_{2,3}$ XMLD with the x-ray beam at 55° off-normal incidence, making only a small angle

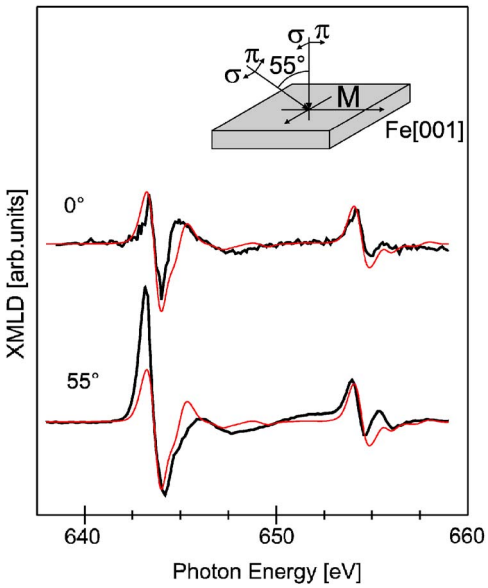


FIG. 4. (Color online) Experimental Mn $L_{2,3}$ XMLD [thick (black) line] for 8 ML MnPt/Fe(100) measured at normal (0°) and grazing (55° off-normal) incidence. The spectra are shifted vertically and are compared to theoretical calculations [thin (red) line] with $10Dq = 0.15$ eV. The inset shows the experimental geometry.

with the substrate magnetization $M$ (Fig. 4). This grazing incidence geometry makes the XMLD sensitive to the anisotropy in the plane normal to $M$, and hence measures the AFM spin orientation in that plane. Both the overall shape and magnitude of the XMLD obtained at 55° off-normal incidence resemble those for normal incidence. The maximum of the $L_3$ XMLD is larger while the other features are similar in size. In the $L_2$ region the first feature is slightly enhanced, and the second one is more pronounced. If the Mn spins were aligned along $M$ then the magnitude of the XMLD for 55° would be three times smaller than that for 0°.[33] The results clearly show that the AFM domains are mainly in the surface plane and perpendicular to $M$, and that out-of-plane spin orientation is quite small.

The magnitude of the theoretical dichroism is about six times larger than the experimental result, which could have several causes. First of all, the theoretical XMLD is obtained for Mn $d^5$ atoms with a magnetic moment of $5\mu_B$, which exceeds the value of $4.3\mu_B$ expected for MnPt at room temperature. The magnitude of the XMLD depends mainly on $\langle M^2 \rangle$, since for $d^5$ in the cubic symmetry the contribution of the charge quadrupole moment is negligible; however, a reduction in $\langle M^2 \rangle$ by a factor of 6 seems hard to explain if all moments are perfectly aligned antiferromagnetically.

Another possible reason for the reduced XMLD could be the presence of uncompensated spins at the AFM/FM interface belonging to the AFM material which results in a net ferromagnetic orientation. This can be probed with XMCD, and the results are shown in Fig. 5. The Mn $L_{2,3}$ spectra were collected with the incident x rays at 45° to the direction of the applied magnetic field. The absence of any visible XMCD signal for Mn confirms the AFM nature of the MnPt film and the absence of any interplay with substrate which could induce FM ordering of the Mn atoms, e.g., due to deep

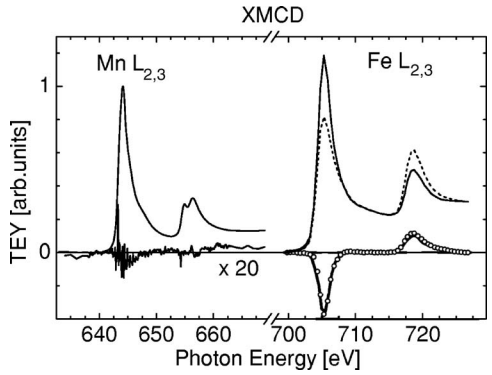


FIG. 5. XAS and XMCD measured at 45° incidence angle with the magnetization direction. The Mn XAS line shape is averaged over the two spectra measured with opposite circular polarizations and it is identical to that of Fig. 2. Fe dichroic spectra were normalized to the average absorption at the maximum of the $L_3$ edge. Fe XMCD for the bare substrate (solid line) is compared with that obtained after MnPt deposition (circles).

intermixing and/or alloying at the interface.[36,37] Moreover the overlayer thickness was chosen to still have a detectable TEY signal from the substrate. The XMCD measured at the Fe $L_{2,3}$ edges shown in Fig. 5 agrees with the values reported in the literature for the bulk,[34] from which we can infer the persistance of a single-domain magnetic structure for the underlying substrate even after the MnPt deposition. We note that the interface region strongly contributes to the Fe XMCD because the sampling depth of the TEY signal (determined by the electron inelastic mean free path) is ~50 Å,[35] and the interface is ~15 Å deep; thus the sensitivity to the arrangement of the Fe magnetic moments at the interface is enhanced.

The persistance of the $(1\times1)$ LEED pattern supports these considerations. However, the role of local defects is essential for the AFM/FM systems. The microscopic Heisenberg model developed in Ref. 6 shows that for perfectly flat, compensated interfaces the spin-flop coupling does not lead to exchange bias but rather to uniaxial anisotropy, while exchange bias strongly depends on the presence of volume defects such as atomic vacancies. Recent experimental[38] and theoretical[39,40] work about AFM-FM coupling for AFM transition metal oxides investigated the consequences of interfacial defects. Provided that such models could apply even to the compensated MnPt/Fe interface, the reduced XMLD can be explained through the presence of dislocations which disrupt the in-plane coherency of the spin-flop state.

## IV. CONCLUSIONS

In conclusion, the combined experimental and theoretical analysis of the epitaxial interface MnPt/Fe(100) enabled us to identify an in-plane orientation of the Mn magnetic moments driven by a spin-flop mechanism leading to a dominant orientation of the AFM domains perpendicular to the substrate magnetization. The absence of uncompensated spins is confirmed by the XMCD measurements. It is tempting to associate the absence of pinning configurations with the presence of a sharp interface, as produced by ideal epitaxial growth.

## ACKNOWLEDGMENTS

We would like to thank M. Fabrizioli and A. Stollo for participating in the experiment. This work was supported by INFM-CNR.

*Electronic address: panaccioneg@elettra.trieste.it

[1] J. Nogues and I. K. Schuller, J. Magn. Magn. Mater. **192**, 203 (1999).
[2] A. E. Berkovitz and K. Takano, J. Magn. Magn. Mater. **200**, 552 (1999).
[3] D. Mauri, H. C. Siegmann, P. S. Bagus, and E. Kay, J. Appl. Phys. **62**, 3047 (1987).
[4] A. P. Malozemoff, Phys. Rev. B **35**, 3679 (1987).
[5] N. C. Koon, Phys. Rev. Lett. **78**, 4865 (1997).
[6] T. C. Schulthess and W. H. Butler, Phys. Rev. Lett. **81**, 4516 (1998).
[7] W. J. Antel, Jr., F. Perjeru, and G. R. Harp, Phys. Rev. Lett. **83**, 1439 (1999).
[8] T. P. A. Hase, B. D. Fulthorpe, S. B. Wilkins, B. K. Tanner, C. H. Marrows, and B. J. Hickey, Appl. Phys. Lett. **79**, 985 (2001).
[9] H. Ohldag, T. J. Regan, J. Stöhr, A. Scholl, F. Nolting, J. Lüning, C. Stamm, S. Anders, and R. L. White, Phys. Rev. Lett. **87**, 247201 (2001).
[10] H. Ohldag, A. Scholl, F. Nolting, E. Arenholz, S. Maat, A. T. Young, M. Carey, and J. Stöhr, Phys. Rev. Lett. **91**, 017203 (2003).
[11] W. H. Meiklejohn and C. P. Bean, Phys. Rev. **102**, 1413 (1956).
[12] W. H. Meiklejohn, J. Appl. Phys. **33**, 1328 (1962).
[13] P. Blomqvist, K. M. Krishnan, and H. Ohldag, Phys. Rev. Lett. **94**, 107203 (2005).
[14] Y. G. Wang and A. K. Petford-Long, J. Magn. Magn. Mater. **279**, 82 (2004).
[15] J. C. A. Huang, C. C. Yu, and C. H. Lee, J. Appl. Phys. **87**, 4921 (2000).
[16] T. Kume, Y. Sugiyama, T. Kato, S. Iwata, and S. Tsunashima, J. Appl. Phys. **93**, 6599 (2003).
[17] Y. Choi, A. K. Petford-Long, and R. C. C. Ward, J. Appl. Phys. **97**, 10C512 (2005).
[18] A. Mougin, J. Borme, R. L. Stamps, A. Marty, P. Bayle-Guillemaud, Y. Samson, and J. Ferré, Phys. Rev. B **73**, 024401 (2005).
[19] E. Kren, G. Kadar, L. Pal, J. Solyom, P. Szabo, and T. Tarnoczi, Phys. Rev. **171**, 574 (1968).
[20] K. O. Legg, F. Jona, D. W. Depsen, and P. M. Marcus, Surf. Sci. **66**, 25 (1977).
[21] M. R. Scheinfein, J. Unguris, J. L. Blue, K. J. Coakley, D. T. Pierce, R. J. Celotta, and P. J. Ryan, Phys. Rev. B **43**, 3395

(1991).
[22] J. Kessler, *Polarized Electrons* (Springer-Verlag, Berlin, 1985).
[23] H. C. Siegmann, D. Mauri, D. Scholl, and E. Kay, J. Phys. (Paris), Colloq. **49**, C8-9 (1988).
[24] F. Sirotti, G. Panaccione, and G. Rossi, Phys. Rev. B **52**, R17063 (1995).
[25] W. L. O'Brien and B. P. Tonner, Phys. Rev. B **51**, 617 (1995).
[26] H. A. Dürr, G. van der Laan, D. Spanke, F. U. Hillebrecht, and N. B. Brookes, Phys. Rev. B **56**, 8156 (1997).
[27] J. Dresselhaus, D. Spanke, F. U. Hillebrecht, E. Kisker, G. van der Laan, J. B. Goedkoop, and N. B. Brookes, Phys. Rev. B **56**, 5461 (1997).
[28] R. D. Cowan, *The Theory of Atomic Structure and Spectra* (University of California Press, Berkeley, 1981).
[29] G. van der Laan and B. T. Thole, Phys. Rev. B **43**, 13401 (1991).
[30] For the Mn $d^5$ configuration the spin-orbit interaction is $\zeta(d)=0.040$ eV and the Slater integrals are $F^2(d,d)=10.316$ and $F^4(d,d)=6.412$ eV. For the Mn $2p^53d^9$ configuration $\zeta(2p)=6.846$, $\zeta(d)=0.053$, $F^2(d,d)=11.155$, $F^4(d,d)=6.941$, $F^2(p,d)=6.321$, $G^1(p,d)=4.606$, and $G^3(p,d)=2.618$ (all in eV) (Ref. 29). Interatomic screening and mixing with other configurations were taken into account by reducing the Slater integrals to 72%. The $2p$ spin-orbit interaction was scaled to 103%. An exchange field of $\mu_B H=0.01$ eV was applied along the magnetization direction. The calculations include a Lorentzian of 0.3 (0.4) eV for the $L_3$ ($L_2$) edge to account for intrinsic linewidth broadening and a Gaussian of $\sigma=0.2$ eV for instrumental broadening.
[31] S. Czekaj, F. Nolting, L. J. Heyderman, P. R. Willmott, and G. van der Laan, Phys. Rev. B **73**, 020401(R) (2006).
[32] C. Grazioli, D. Alfe, S. R. Krishnakumar, S. S. Gupta, M. Veronese, S. Turchini, N. Bonini, A. Dal Corso, D. D. Sarma, S. Baroni, and C. Carbone, Phys. Rev. Lett. **95**, 117201 (2005).
[33] G. van der Laan, Phys. Rev. Lett. **82**, 640 (1999).
[34] R. Nakajima, J. Stöhr, and Y. U. Idzerda, Phys. Rev. B **59**, 6421 (1999).
[35] W. L. O'Brien and B. P. Tonner, Phys. Rev. B **50**, 12672 (1994).
[36] N. I. Kulikov and C. Demangeat, Phys. Rev. B **55**, 3533 (1997).
[37] P. Torelli, F. Sirotti, and P. Ballone, Phys. Rev. B **68**, 205413 (2003).
[38] M. Finazzi, M. Portalupi, A. Brambilla, L. Duo, G. Ghiringhelli, F. Parmigiani, M. Zacchigna, M. Zangrando, and F. Ciccacci, Phys. Rev. B **69**, 014410 (2004).
[39] M. Finazzi, Phys. Rev. B **69**, 064405 (2004).
[40] M. Finazzi, P. Biagioni, A. Brambilla, L. Duo, and F. Ciccacci, Phys. Rev. B **72**, 024410 (2005).